Synthesis of nanoscale composites of exchange biased $MnFe_2O_4$ and Mn-doped $BiFeO_3$

C.-H. Yang, F. Yildiz, S.-H. Lee, Y. H. Jeong, U. Chon et al.

Citation: Appl. Phys. Lett. **90**, 163116 (2007); doi: 10.1063/1.2724909
View online: http://dx.doi.org/10.1063/1.2724909
View Table of Contents: http://apl.aip.org/resource/1/APPLAB/v90/i16
Published by the American Institute of Physics.

Synthesis of nanoscale composites of exchange biased $MnFe_2O_4$ and Mn-doped $BiFeO_3$

C.-H. Yang, F. Yildiz, S.-H. Lee, and Y. H. Jeong[a)]
Department of Physics, Pohang University of Science and Technology, Pohang 790-784, Korea

U. Chon
Research Institute of Industrial Science and Technology, Pohang 790-330, Korea

T. Y. Koo
Pohang Accelerator Laboratory, Pohang University of Science and Technology, Pohang 790-784, Korea

(Received 5 December 2006; accepted 16 March 2007; published online 19 April 2007)

Exchange bias may be used to couple a normal ferromagnet to a ferroelectric antiferromagnet and thus create a multiferroic system with nonzero magnetization. In implementing this idea the authors developed a synthesis method for composite films of nanoscale clusters of ferromagnetic $MnFe_2O_4$ embedded in multiferroic Mn-doped $BiFeO_3$. The method utilizes the Bi volatility to obtain the composite films via thermal annealing of multilayers composed of $BiFeO_3$ and $BiMnO_3$. The cluster size varies from 20 to 80 nm depending on the film thickness. The composite films possess both ferroelectric and ferromagnetic properties; the magnetic hysteresis curves, in particular, manifest exchange bias. © *2007 American Institute of Physics*. [DOI: 10.1063/1.2724909]

Multiferroic materials are being vigorously studied due to their application potentials utilizing the magnetoelectric (ME) effect, which is the induction of magnetization/polarization with an applied electric/magnetic field.[1–3] Most significant multiferroics turned out to be ferroelectric antiferromagnets such as $BiFeO_3$. Since antiferromagnets are of limited value in applications, ferroelectric ferromagnets are desired; however, this kind of materials are not common. Multiferroic $BiMnO_3$ may be a rare example with a large saturated magnetization of $3.6\mu_B$/Mn, but this material has a rather low magnetic Curie temperature ($T_C \sim 105$ K).[4]

To circumvent the problem, there have been efforts to utilize *exchange bias*.[5,6] Exchange bias refers to the phenomenon occurring in ferromagnet/antiferromagnet heterojunctions, where the exchange interaction through the interface causes magnetization to possess a preferred direction and the *M-H* (magnetization versus magnetic field) curve to shift to the negative side. Consider a composite material consisting of a ferroelectric antiferromagnet and a normal ferromagnet. If exchange bias is in operation in the composite and a ME coupling is present in the antiferromagnetic multiferroic, the magnetization mostly from the ferromagnet would become controllable.

Here we wish to report our efforts to implement exchange bias to enhance the magnetization change; composite structures composed of multiferroic Mn-doped $BiFeO_3$ and ferromagnetic $MnFeO_4$ were attempted and to this end a synthesis method was developed. $MnFeO_4$ is a ferromagnet with $T_C \sim 573$ K. $BiFeO_3$ has ferroelectric $T_C \sim 1110$ K and antiferromagnetic $T_N \sim 643$ K; the magnetic order is basically of *G* type (all neighboring ions couple antiferromagnetically) with a spiral modulation.[7] Mn doping to $BiFeO_3$ has an effect of decreasing T_N.[8]

The synthesis method we developed takes advantage of self-assembly of nanoscale structures with resultant large interface areas between the two materials.[9–11] The method takes advantage of the well-known volatility of Bi ions. We first deposited $[BiFeO_3/BiMnO_3]_n$ multilayer thin films using the pulsed laser deposition technique on $SrTiO_3(100)$ substrates. $BiFeO_3$ was grown for 2 min and $BiMnO_3$ was deposited for another 2 min successively; this bilayer was repeated for *n* times. The wavelength, pulse rate, and fluence of the laser were 266 nm, 4 Hz, and 2.5 J/cm^2, respectively. The substrate temperature was 585 °C and oxygen pressure was 3 mTorr. Postannealing treatments were done for 90 min at the same temperature and oxygen pressure. The volatility of Bi ions caused part of Bi ions to be lost from the multilayer during both growing and postannealing periods. Then consequent extra Mn and Fe ions induced a stable spinel phase $MnFe_2O_4$. A variety of films with different *n* was made and characterized. In what follows we shall present various measurements carried out on two representative samples with $n=40$ and 10, which are denoted as S40 and S10, respectively.

It is noted that the deposition of $BiFeO_3$ alone without $BiMnO_3$ did not lead to a second phase under the same conditions. It is also noted that pure $BiMnO_3$ thin films could not be obtained above 500 °C due to Bi evaporation;[12,13] excess bismuth in the target was required for $BiMnO_3$ thin films at high temperatures. These results indicate that $BiFeO_3$ is more stable against Bi loss.

First of all, surface morphology and cross-section images were examined by scanning electron microscopy (SEM) and atomic force microscopy (AFM). The thicknesses of S40 and S10 were estimated, using the cross-sectional SEM image and deposition time, to be 130 and 32 nm, respectively. In Figs. 1(a) and 1(b) presented are the SEM surface images of S40 and S10, respectively; the lateral direction is along the substrate [100] direction. From Fig. 1(a) the coexistence of two phases, loosely connected clusters, and underlying matrix region is observed. The typical size of the clusters is about 80 nm and the edge direction of the rectangular cluster is parallel to the substrate [110] direction. Figure 1(b) shows uniformly packed clusters residing in the matrix. The typical

[a)]Electronic mail: yhj@postech.ac.kr

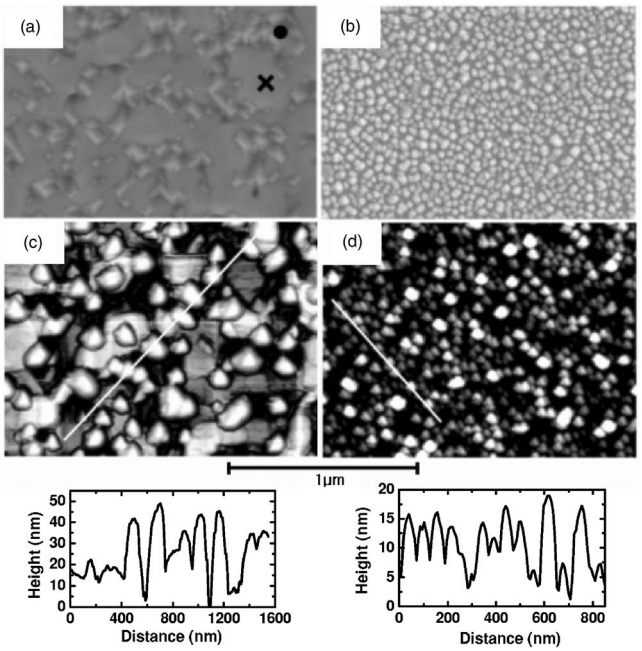

FIG. 1. SEM and AFM images for surface morphology of the composite films: (a) and (c) for S40 and (b) and (d) for S10. (a) and (b) are from SEM and (c) and (d) from AFM. Figures show that the two phases of the clusters and background coexist in the films. From AFM scanning along the lines indicated in (c) and (d), height variation shown is obtained. Local EDX analysis reveals that the clusters in (a) marked by a solid circle does not contain Bi, whereas the cross marked region does.

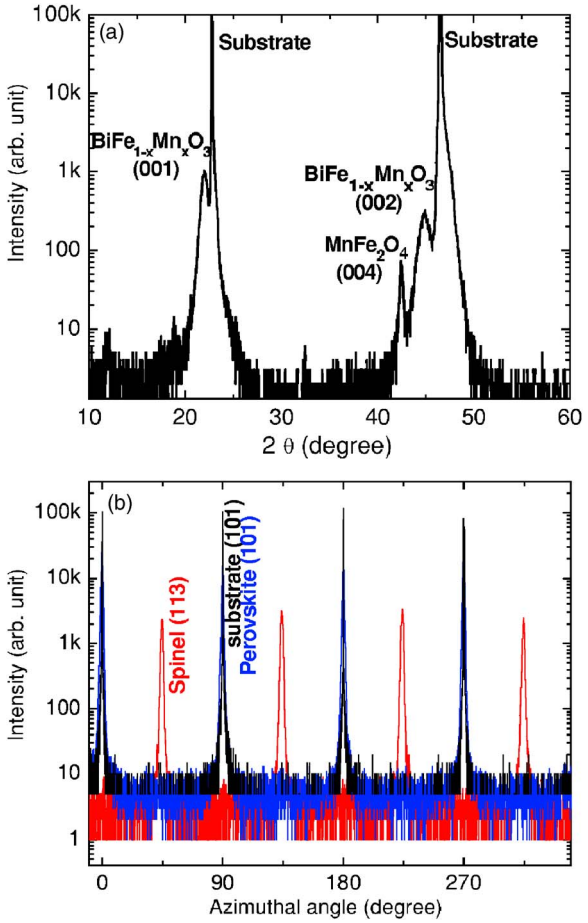

FIG. 2. (Color online) X-ray diffraction results for the composite film S10. (a) θ-2θ scan revealing the existence of two phases. (b) Azimuthal scans with respect to the film normal for the representative peaks of the spinel phase, the perovskite phase, and the substrate.

cluster size in this case is around 40 nm. The AFM images, Figs. 1(c) and 1(d) for S40 and S10, respectively, presented with the corresponding height variation, also show similar features as those of SEM except that the AFM images may contain tip convolution effects. While the typical cluster size of S10 is around 40 nm, it decreases down to about 20 nm for a very thin $n=4$ film. These results show that the typical size of the clusters in the composite films is strongly related to the film thickness, which in turn means that one can control the cluster size. It should be pointed out that the peculiar morphology displayed in Fig. 1(a) occurred only when the film thickness is larger than the consequent cluster size, while the type of Fig. 1(b) is generally seen in the opposite cases.

In order to identity the two phases of the composite films, local energy dispersive x-ray (EDX) analysis and x-ray diffraction (XRD) measurements were performed. The EDX analysis, as indicated in Fig. 1(a), revealed an important fact that no Bi exists in the cluster region in contrast to the Bi containing matrix region. As for the XRD measurements, Fig. 2(a) is the θ-2θ scan for S10; similar results were obtained for the films with different n. Note that only two kind of crystalline peaks from the film are observed. From lattice spacing determination the perovskite Mn-doped $BiFeO_3$ and spinel $MnFe_2O_4$ could be assigned to the peaks. Combining this with the SEM/EDX results, the clusters without Bi are identified unequivocally as $MnFe_2O_4$, while Mn-doped $BiFeO_3$ constitutes the matrix. The in-plane crystalline orientations of the two phases are well aligned to the substrate as ascertained from the fourfold symmetry of Fig. 2(b), the azimuthal scan around the film normal. The (101) peaks from the perovskite and substrate coincide, and the spinel (113) peak is 45° off from the perovskite one.

Turning to the physical properties of the composite films, a piezoresponse force microscope (PFM) was used to characterize the ferroelectric properties.[14] Since bottom electrodes are required for this purpose, metallic $SrRuO_3$ buffer layers were first deposited on substrates. A modulation voltage at 17 kHz (amplitude=0.5 V) and a dc bias voltage were applied simultaneously between the probing platinum tip and bottom electrode. In Fig. 3 presented are the piezoelectric responses measured for a film, which is equivalent to S40 in growth and treatment conditions, on a $SrRuO_3/SrTiO_3$ buffered substrate. The PFM amplitude and phase, as a function of bias voltage, show characteristic hysteric behaviors, and this feature is taken as an evidence of ferroelectricity. A slight imprint toward the negative electric field is caused by the inequivalence between the $SrRuO_3$ bottom electrode and the platinum tip. In Fig. 3(c) plotted is a phase contrast mapping with different poling fields; the bright and dark regions represent polarizations pointing up and down along the surface normal, respectively. Negative poling (negative voltage to tip) induced the light region, whereas positive poling gave rise to the dark region.

Next to the PFM measurements, M was investigated as a function of H (in-plane [100] direction) and T (temperature) with a vibrating sample magnetometer. $M(T)$ was obtained during cooling from 350 K under 1 kOe, and the M-H curve at 5 K was measured after field cooling at 1 kOe. Figure 4, the plot of M-H and $M(T)$ for S40 and S10, shows that both

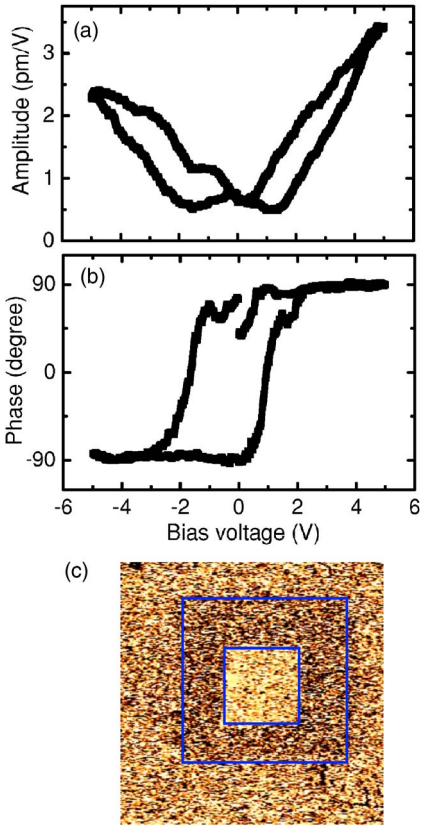

FIG. 3. (Color online) PFM results of the film with a $SrRuO_3$ bottom electrode. The thickness of the film is equivalent to that of S40. (a) The amplitude and (b) phase of the PFM signal are shown as a function of bias voltage. (c) Phase contrast mapping of a 8×8 μm^2 area. The poling voltage was −5 V for the light region in the center and +5 V in the surrounding dark region.

samples exhibit clear ferromagnetism with T_C above room temperature. A relatively large M obtained for S10 is consistent with its high cluster density. The M-H curves, Figs. 4(a) and 4(b), illustrate that the center of the hysteresis loop is shifted toward the negative side and thus indicate that exchange bias is in operation. In Figs. 4(c) and 4(d) presented is M as a function of T; the slight down curvature of the

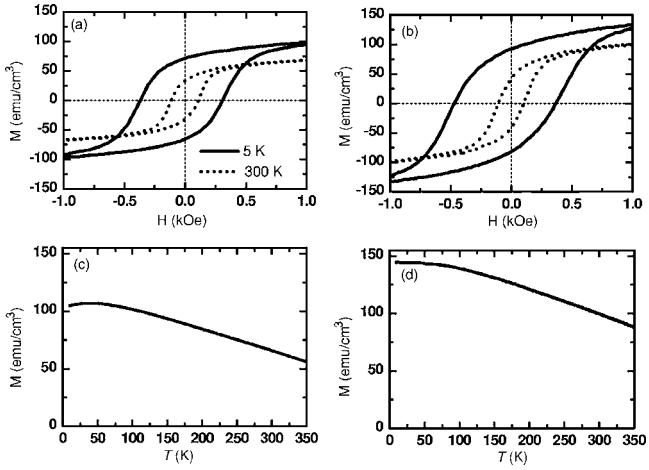

FIG. 4. Magnetic properties of the composite films: (a) and (c) for S40 and (b) and (d) for S10. The applied field direction was in plane. The $M(T)$ curves displayed as (c) and (d) were obtained during cooling from 350 K under 1 kOe. All data are normalized to the entire sample volume (not volume of spinel).

$M(T)$ curves at low temperatures seems to be caused by the blocking behaviors of inevitable superparamagnetic components. Note that M decreases, as T increases, almost linearly above 150 K for both samples.

Of exceeding importance is, of course, to confirm that the intended exchange bias effects are achieved in the composite films. From the M-H curves the coercive fields H_c^L and H_c^R at 5 K (L denotes the left side and R does right) are determined: −369 and 309 Oe for S40 and −470 and 367 Oe for S10. Two quantities are of direct interest, that is, the average coercivity ($H_c^{\mathrm{av}} \equiv |H_c^R - H_c^L|/2$) and the exchange bias ($H_b \equiv |H_c^R + H_c^L|/2$). H_c^{av} is calculated to be 340 Oe for S40 and 418 Oe for S10. The coercivity of S40 and S10 shows the size dependence seen in other magnetic nanoparticles.[15] More importantly, the exchange bias H_b is obtained as −30 and −52 Oe for S40 and S10, respectively. (For a S4 film, −90 Oe was obtained.) Note that while the exchange effect is not extremely large, it does show a negative shift. The variation of H_b with cluster size may be understood from a simple balance of the exchange and magnetostatic energy:[16] $E_{\mathrm{ex}}S \approx MVH_b$, where E_{ex} is the interfacial exchange energy density and S and V are the interface area and volume of the cluster. Then $H_b \propto S/V$ which explains the size dependence. As for the smallness of H_b, it seems to be related to the G-type magnetic order of $BiFeO_3$, whose spin arrangements exposed on the interface are likely to include antiferromagnetic ones. This would then cause partial cancelation of exchange bias effects. Obviously more controlled investigation is needed and under way using bilayer and multilayer films.

In conclusion we developed a method for synthesizing composite films composed of nanoscale clusters of ferromagnetic $MnFe_2O_4$ embedded in multiferroic Mn-doped $BiFeO_3$, and demonstrated the multiferroicity and exchange bias effect of the films.

The authors wish to thank the financial supports from KOSEF (2000-SRC).

[1] M. Fiebig, J. Phys. D **38**, R123 (2005).
[2] S.-W. Cheong and M. Mostovoy, Nat. Mater. **6**, 13 (2007).
[3] R. Ramesh and N. A. Spaldin, Nat. Mater. **6**, 21 (2007).
[4] H. Chiba, T. Atou, and Y. Syono, J. Solid State Chem. **132**, 139 (1997).
[5] J. Dho, X. Qi, H. Kim, J. L. MacManus-Driscoll, and M. G. Blamire, Adv. Mater. (Weinheim, Ger.) **18**, 1445 (2006).
[6] V. Laukhin, V. Skumryev, X. Marti, D. Hrabovsky, F. Sanchez, M. V. Garcia-Cuenca, C. Ferrater, M. Varela, U. Luders, J. F. Bobo, and J. Fontcuberta, Phys. Rev. Lett. **97**, 227201 (2006).
[7] I. Sosnowska, T. Peterlin-Neumaier, and E. Steichele, J. Phys. C **15**, 4835 (1982).
[8] C.-H. Yang, T. Y. Koo, and Y. H. Jeong, Solid State Commun. **134**, 299 (2005).
[9] H. Zheng, J. Wang, S. E. Lofland, Z. Ma, L. Mohaddes-Ardabili, T. Zhao, L. Salamanca-Riba, S. R. Shinde, S. B. Ogale, F. Bai, D. Viehland, Y. Jia, D. G. Schlom, M. Wuttig, A. Roytburd, and R. Ramesh, Science **303**, 661 (2004).
[10] H. Zheng, F. Straub, P. Yang, W. Hsieh, Z. Florin, Y. Chu, U. Dahmen, and R. Ramesh, Adv. Mater. (Weinheim, Ger.) **18**, 2747 (2006).
[11] C.-W. Nan, G. Liu, Y. Lin, and H. Chen, Phys. Rev. Lett. **94**, 197203 (2005).
[12] C.-H. Yang, T. Y. Koo, S.-H. Lee, C. Song, K.-B. Lee, and Y. H. Jeong, Europhys. Lett. **74**, 348 (2006).
[13] W. Eerenstein, F. D. Morrison, J. F. Scott, and N. D. Mathur, Appl. Phys. Lett. **87**, 101906 (2005).
[14] A. Gruverman, O. Auciello, and H. Tokumoto, Annu. Rev. Mater. Sci. **28**, 101 (1998).
[15] F. E. Luborsky, J. Appl. Phys. **32**, S171 (1961).
[16] A. E. Berkowitz and K. Takano, J. Magn. Magn. Mater. **200**, 552 (1999).